Fachtagung "Experimentelle Strömungsmechanik"
7.–9. September 2021, Bremen

Prevention and Inhibition of Foam in Packed Columns: Interface Stability and Flow Properties

N. Topic[1], H. Hohagen[1], L. Almazán-Torres[1], A. Osorio-Nesme[1] and A. Delgado[1,2]

[1]LSTM, Friedrich-Alexander-Universität Erlangen-Nürnberg, Erlangen/Germany
[2]German Engineering Development and Research Center LSTME Busan/South Korea

Foam prevention, Instability, Flow profiles, Optical measurements

Abstract

In this work, we consider prevention and inhibition of foams in packed columns through systematic studies of the stability of fluid dynamic processes in simplified channels. For the analytical analysis, we consider liquids that are initially stationary in a channel. Then a localized quasistatic perturbation normal to the interface is applied and the stability of the interface is analyzed. We also consider the case of a liquid flowing in a channel and calculate the surface profiles in dependence on the flow rate. Finally, we compare the results with experiments.

Introduction

The utility of packed columns stems from their ability to efficiently exchange matter between a gas and a liquid phase. Applications include extraction, absorption, distillation, and rectification, [Billet and Schultes 1999]. Foams can be detrimental in industrial treatment and production plants and can even cause their failure. Therefore, avoiding, inhibiting, as well as actively destructing foams is under active research [Winterburn et al. 2009, Rodríguez et al. 2010, Anderl et al. 2014, Gallego-Juárez et al. 2015, Vaidya et al. 2016, McHardy et al. 2018, Thünnesen et al. 2019, Gatternig et al. 2019]. In this work, we consider geometrical surfaces in which the process of bubble formation cannot exist or is strongly inhibited and present the flow characteristics in the channels, studied theoretical and experimentally.

The perturbation of the liquid interface in the normal direction has been shown to be one of the causes of bubbles, and hence, foam formation, [Wei et al. 2017]. To study this process analytically, we consider liquids that are initially stationary in a channel. We then apply a localized quasistatic perturbation normal to the interface and consider its stability. The criterion for the stability of the initial surface is based on the variational approach [Roy and Schwartz 1999]. For the stability of the final configuration we focus on the breakup into droplets as such instability may also cause bubble entrapment, e.g. by collisions [Tran et al. 2013]. We use the conditions for the non-existence of droplets developed by Concus et al. [Concus et al. 2001, Han et al. 2019].

Channels with triangular cross-sections often appear in packed columns [Olenberg et al. 2018]. The flow in channels with triangular cross-sections was first treated semi-analytically by Sparrow [Sparrow 1962]. This method was recently applied to the case where one side is a free surface, imposing no-shear stress boundary conditions [Almazán et al. 2019]. Here we derive improved free surface profiles and compare with experimental data.

For the measurements, we perform a systematic experimental study of a liquid flow in triangular channels for various channel opening angles, channel inclinations and flow rates. The interface profiles at a representative cross-section are obtained by means of optical image analysis with the help of Laser sheets.

Stability of the interface

The studied channel is considered horizontal and its length is assumed much larger than its characteristic width. The initial resting fluid forms a characteristic concave meniscus due to the constant contact angle γ with the walls. The Bond number $Bo = (\rho_l - \rho_g) g \Delta h^2 / \sigma$ is assumed to be much smaller than 1, where ρ_l and ρ_g are the densities of the liquid and gas phases, g is the gravity, σ the surface tension and Δh the characteristic length of the interface. Hence, the surface can be approximated as cylindrical. For the purposes of calculation, we will consider a section of the channel of length L, as shown in Figure 1.

The stability of this kind of surface to infinitesimal perturbations has been considered previously [Roy and Schwartz 1999]. A stability condition $\frac{dp}{dA} > 0$ was derived, where p is the pressure corresponding to the meniscus of the liquid (positive for convex and negative for concave surface, with liquid designating the interior) and A is the cross-sectional area of the liquid on the *yz* plane. As $\frac{dp}{dA} > 0$ for concave surfaces in triangular channels, it follows that the surfaces are stable to infinitely small perturbations. Therefore, as initial surfaces subjected to a perturbation, we consider only the concave profile. For a given contact angle γ the surfaces are concave for $\frac{\alpha}{2} + \gamma < \pi/2$, where α is the channel opening angle measured from wall to wall.

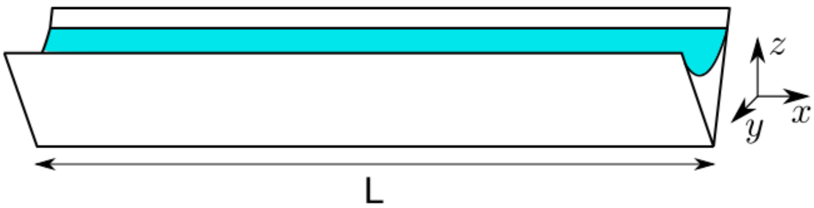

Figure 1: Initial state of the liquid in a triangular channel.

The liquid flowing in a channel inside of a packed column may be subjected to a variety of perturbations, such as air flow over its free surface. The velocity of the liquid can also act as a perturbation at the liquid-gas interface, depending on its magnitude. Hence, although the surface itself is stable, a finite-magnitude perturbation may destabilize it, which can lead to formation of bubbles and foam. Therefore, in the present analysis a perturbation normal to the surface is applied. The amount of energy ΔE needed to reach an unstable configuration is then calculated. This energy is used as a measure of the stability of the surface.

Figure 2(a) shows the initial configuration of the studied channel. The perturbation is assumed to be uniformly applied as a plane along the x-direction of the channel in the geometrical middle at $y = 0$. Such choice of perturbation allows an analytical description. We considered other types of perturbations, e.g. a point like disturbance, but we did not find an analytical solution. Initially, the plane is outside of the liquid. As the plane moves into the liquid the surface will deform as shown in Figure 2(b). For the case when the contact angle formed with the perturbing plane is smaller than $90°$ the interface will deform, even before the plane enters into the fluid. Once the plane enters the liquid, Figure 2(c), the free surface shows a constant contact angle ϕ with it. In the final configuration, the plane is pushed until the bottom of the channel. The cross-sectional area A of the liquid remains constant.

The stability of the final configuration, Figure 2(c) can be analyzed with the help of the condition where droplets cannot exist in the channel if $\gamma + \phi + \alpha/2 < \pi$ [Concus et al. 2001]. The critical angle formed by the perturbing plane is that when the interface exhibit a perfect flat surface, i.e. when $\gamma + \phi + \frac{\alpha}{2} = \pi$, the sum of the internal angles in a triangle. With this critical configuration, we can find the energy needed to reach the critical state for instability.

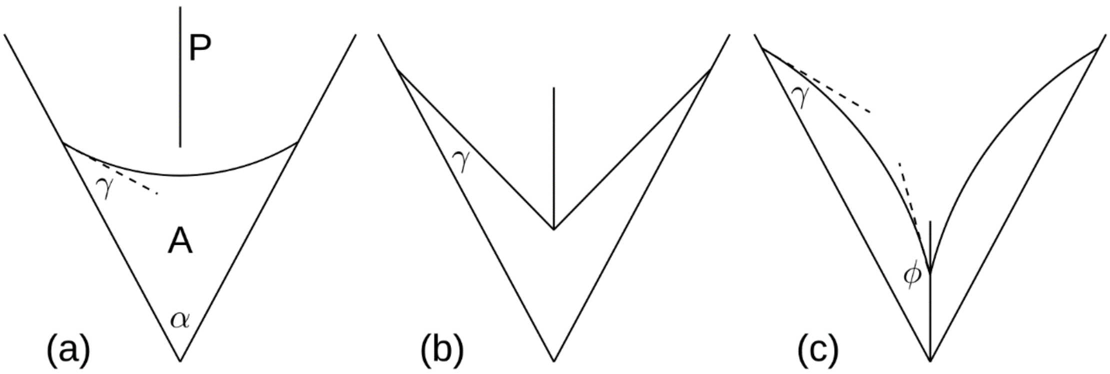

Figure 2: Deformation of the interface subjected to a perturbing plane P.

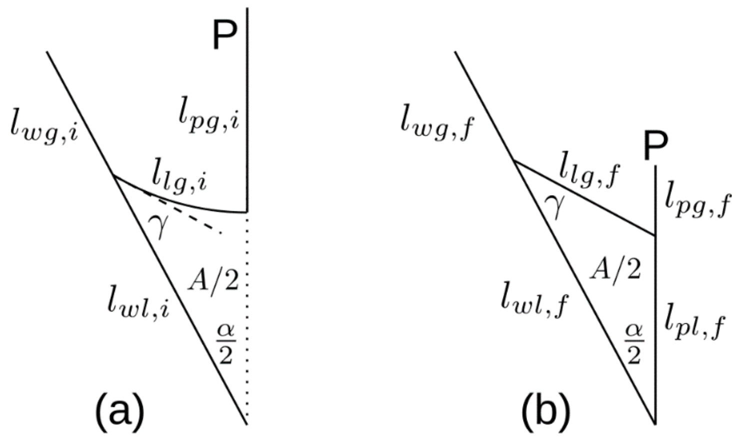

Figure 3 : The lengths of the interfaces in the initial stable state (a) and the final critical state (b).

Due to symmetry, we consider only half channels. The Figure 3(a) shows the initial configuration, while the Figure 3(b) shows the final stage. The change in energy between configurations (a) and (b) in Figure 3 can be approximated by

$$\Delta E_{1/2} = \sigma \Delta S_{lg} + (\sigma_{wl} - \sigma_{wg})\Delta S_{wl} + (\sigma_{pl} - \sigma_{pg})\Delta S_{pl},$$

where subscript 1/2 refers to the half of the channel ($\Delta E = 2\Delta E_{1/2}$), σ is the surface energy, S is the interface area. Subscripts w, l, g and p indicate wall, liquid, gas, and plane, respectively. Pairs of indices indicate an interface, e.g wl is the interface between the wall and the liquid. Exception is σ without a subscript that corresponds to liquid-gas surface tension. The previous equation can be rewritten with the help of the Young relation,

$$\Delta E_{1/2} = \sigma L(\Delta l_{lg} - \cos(\gamma)\, \Delta l_{wl} - \cos(\phi) l_{pl})$$

where $\Delta l_{lg} = l_{lg,f} - l_{lg,i}$, $\Delta l_{wl} = l_{wl,f} - l_{wl,i}$ with quantities l with subscripts as in Figure 3. The equation can be written in a non-dimensional way as follows:

$$\Delta E_{1/2} = \sigma L A^{1/2}(\Delta l_{lg}^* - \cos(\gamma)\,\Delta l_{wl}^* - \cos(\phi) l_{pl}^*)$$

where * indicates that a length is divided by $A^{1/2}$, which in this case is the total cross-sectional area of the liquid.

To calculate the lengths (as a general symbol we use l) in Figure 3, we first find the dependence $A(l, \alpha, \gamma)$. We then invert those relations to obtain $l(A, \alpha, \gamma)$, and then substitute those expressions into the expression for the change in energy. The quantities are as follows:

$$l_{lg,i} = A^{1/2}\sqrt{\frac{\delta^2}{\sin(\delta)\left(\cos(\delta) + \sin(\delta)\cot\left(\frac{\alpha}{2}\right)\right) - \delta}}$$

$$l_{lg,f} = A^{1/2}\sqrt{\frac{2}{2\sin^2(\theta)\cot\left(\frac{\alpha}{2}\right) - \sin(2\theta)}}$$

$$l_{wl,i} = A^{1/2}\sqrt{\frac{2}{(\cos(\alpha/2) + \sin(\alpha/2)\cot(\delta))\sin\left(\frac{\alpha}{2}\right) - \frac{\sin^2(\frac{\alpha}{2})}{\sin^2(\delta)}\delta}}$$

$$l_{wl,f} = A^{1/2}\sqrt{\frac{2}{\sin(\alpha) - 2\sin^2(\alpha/2)\cot(\theta)}}$$

$$l_{pl} = A^{1/2}\sqrt{\frac{1}{\sin(\alpha/2)\left(\cos\left(\frac{\alpha}{2}\right) + \sin(\alpha/2)\cot(\gamma)\right)}}$$

where $\delta = \frac{\pi}{2} - (\gamma + \alpha/2)$ and $\theta = \gamma + \alpha/2$.

We now use the dependence of the energy needed to destabilize the interface to evaluate how stable is the original, unperturbed, surface. Figure 4 shows the dependence of the non-dimensionalized ΔE on the system properties α and γ. From Figure 4 one can observe that the curves for smaller contact angles ($\gamma = 1°, \gamma = 10°$) are above the ones for larger angles, regardless of the channel opening (α). Hence, the reduction of contact angle improves stability of the interface. As the channel opening angle reaches its maximal possible value for a given contact angle, $\alpha = \pi - 2\gamma$, in order for the initial surface to be stable, the energy for destabilization tends to zero regardless of the contact angle. Finally, for the decreasing channel opening angle the energy increases indicating a more stable interface.

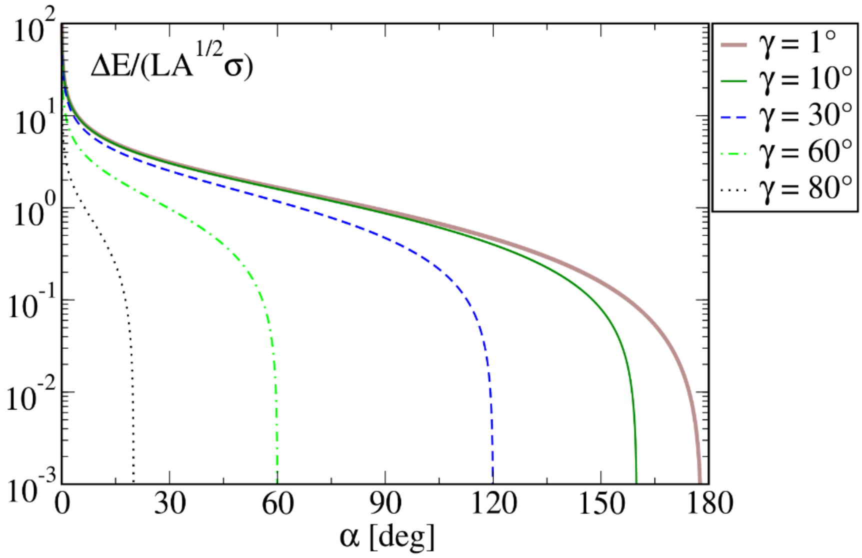

Figure 4: Dependence of energy needed to reach the boundary of the non-existence on the system properties.

Relation between flow rate and interface profile

We now consider the liquid flowing in a channel from Figure 1, but with an inclination β with the horizontal. We assume again that the gravity does weakly influence the surface profile, that is, the Bond number is much smaller than 1. In this case the interface profile is almost cylindrical, attached to the channel walls with a defined contact angle. The cross-sectional area, and therefore the interface profile is then determined by the flow rate Q. We now calculate the flow rate by finding the velocity profile.

For a flow in a triangular channel with fully-developed and laminar flow the Navier-Stokes equation reduces to [Sparrow 1962, Almazán et al. 2019]

$$\Delta u = \frac{\rho g \sin\beta}{\mu}$$

where u is the velocity of the liquid along the channel, g is the gravitational acceleration and μ is the viscosity. For this case, we use a polar coordinate system, where ξ is the polar angle of the channel with $r = 0$ corresponding to the intersection of the walls. By using the separation of variables, the solution can be expanded, and together with no slip boundaries at the walls $\xi = \pm\alpha/2$ gives [Sparrow 1962, Almazán et al. 2019]

$$u = \frac{\rho g \sin\beta}{\mu}\frac{r^2}{4}\left(1 - \frac{\cos(2\xi)}{\cos(\alpha)}\right) + \sum_{n\geq 1} A_n r^{\frac{2n-1}{\alpha}} \cos\frac{2n-1}{\alpha}\xi.$$

The coefficients A_n are found from the no-shear stress condition at the liquid-gas interface. The condition is observed in a number of points n_p. Assuming trucation of the series such that $n = n_f$ is the largest n in the expansion, and with $n_p = n_f$ the boundary condition at the interface becomes a $n_p \times n_p$ linear system of equations for the coefficients A_n. Here, we use an overdetermined system $n_p > n_f$, and find the optimal coefficients.

For a given surface of the liquid the velocity profile is calculated and the volume flow rate is

$$Q = \int_A u \, ds$$

where ds is the element of the cross-sectional area. As in the experiments, the flow rate is the controlled parameter and the position of the interface profile is not known in advance, we vary the interface profile until the predicted flow rate matches the value used in the experiments.

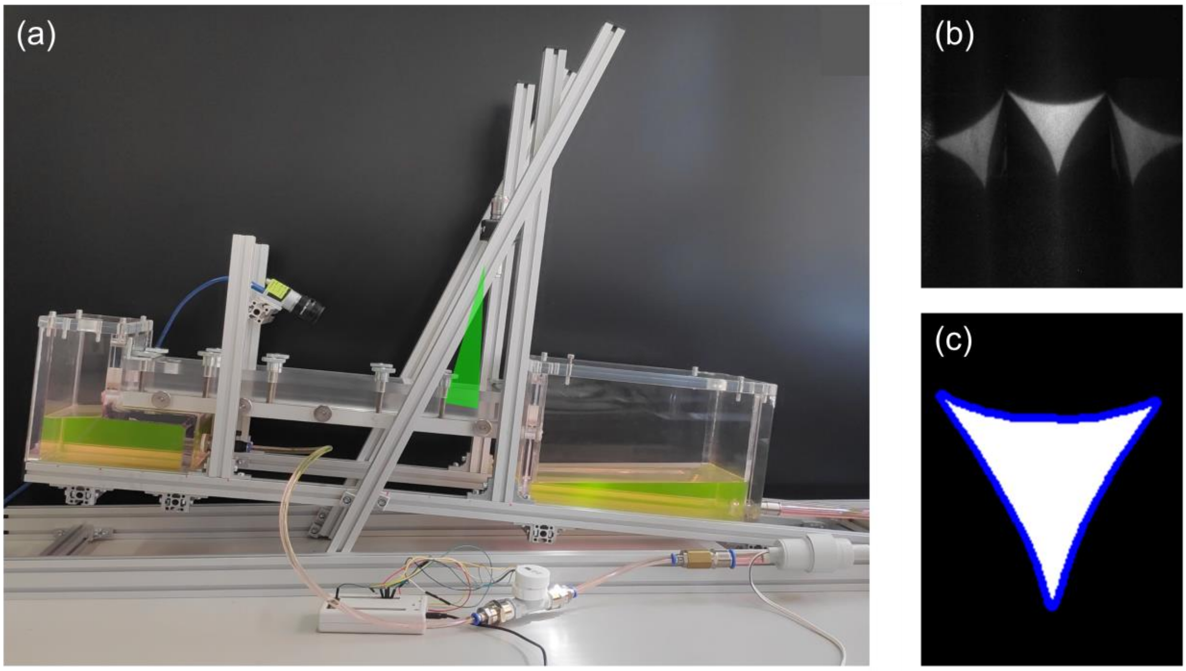

Figure 5: (a) Experimental setup, (b) recorded image of the cross section and (c) the extracted cross section.

Additionally, we performed experimental measurements of water flowing in an inclined channel and compare the final liquid interface profile at a specific cross-section with the theory. The side walls of the channel were of Plexiglas. The channel has a length of 50 cm and is inclined $\beta = 10°$. Two channels with opening angles of $15°$ and $30°$ were used for flow rates of $\mathrm{Q} = 1.67\ \mathrm{cm}^3/\mathrm{s}$, $\mathrm{Q} = 3.33\ \mathrm{cm}^3/s$ and $\mathrm{Q} = 5\ \mathrm{cm}^3/\mathrm{s}$. The interface profile was obtained by shining a laser sheet through the cross section of the liquid. The cross section was made visible by adding Rhodamine 6G fluorescent dye to distilled water as seen in Figure 5(a). Images were taken of the cross section and the surface profile was extracted as seen in Figures 5(b) and (c). The height of the pictures was adjusted to compensate the camera angle. The cross-section for the measurements was located 5 cm from the channel exit. For each flow rate and channel opening angle 3 measurements were conducted and the results were averaged. Figure 6 shows the interface profiles predicted theoretically compared with those from the measurements for both opening angles of the channel and different flow rates and $\beta = 10°$. The temperature was assumed to be $22℃$. The water viscosity used for the theoretical calculations was $9.55 \times 10^{-4}\mathrm{Pa} \cdot \mathrm{s}$. The contact angle for the theory was measured from the experiments and found to be of $57°$.

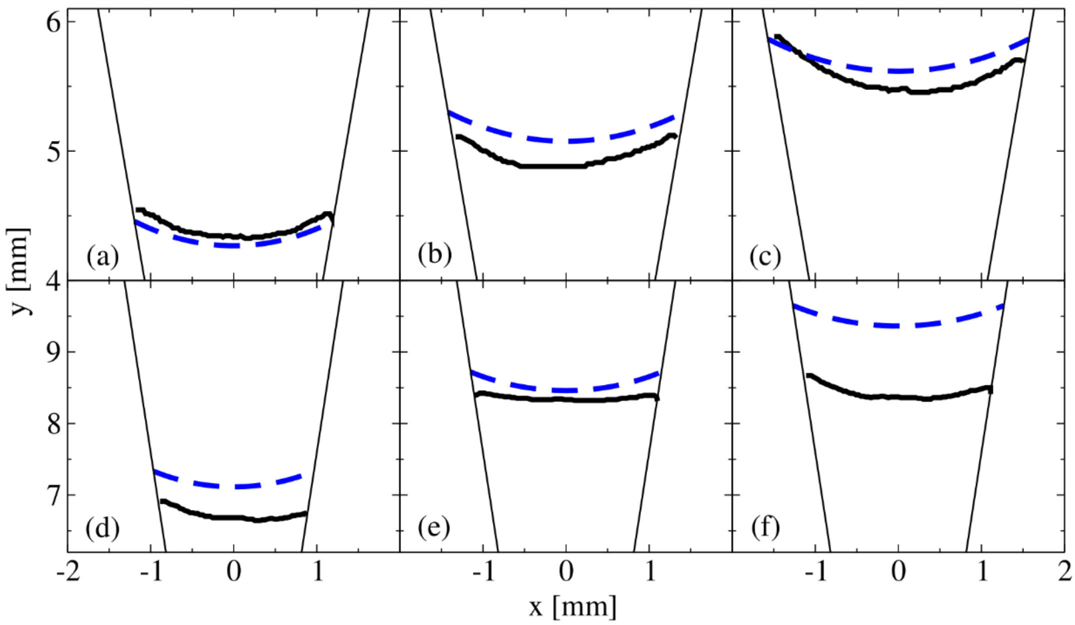

Figure 6: Comparison of the experimentally measured interface profile (black lines), with the predicted interface by the theory (blue lines). Thinner black lines indicate channel walls. The top row corresponds to the channel opening angle of $30°$, while bottom to $15°$. For (a) and (d) $\mathrm{Q} = 1.67\ \mathrm{cm}^3/\mathrm{s}$, (b) and (e) $\mathrm{Q} = 3.33\ \mathrm{cm}^3/\mathrm{s}$, and (c) and (f) $\mathrm{Q} = 5\ \mathrm{cm}^3/\mathrm{s}$. The channel inclination was $\beta = 10°$.

For the channel opening angle of $30°$ we can observe a relatively good agreement between the theory and experiments, especially at low flow rates. On the other hand, for the channel with opening angle of $15°$ there are noticeable deviations between the results. This can be attributed to significant flow fluctuations observed in the experiments. Although the cross-section for the measurements was chosen as far as possible from the inlet to ensure fully-developed flow conditions, the flow was not completely developed. The channel might be too short to create fully-developed flow conditions. Additionally, we also observed some non-negligible flow fluctuations between measurements for the same α and Q. This might be caused by contact angle hysteresis that induces infinitesimal instabilities in the flow. Nevertheless, we observed a good overall agreement between the theoretical solution and experiments.

Conclusions and remarks

In the first part we have analyzed the stability of a static fluid in a triangular channel. We calculated analytically the required energy of a localized perturbation to destabilize an initially stable fluid interface. We found that for both smaller contact angles and channel opening angles the energy for destabilization is larger than for larger contact and opening channel angles, indicating that such interfaces may contribute to prevent bubbles, and hence possible foam formation. This method may also be extended to the case with flow in the channel, however analytical predictions of stability in cases with flow are still subject of research.

In the second part, we predicted theoretically the interface of a fully-developed, steady flow in a triangular channel subjected to an inclination for different flow rates. The predictions were compared with experimental results for similar flow channels considering water. Although there are some deviations between the results caused by induced flow instabilities and unsteadiness, we found a good overall agreement between the theory and experiments.

Acknowledgements

The authors gratefully acknowledge the support given by the German Science Foundation (DFG) with the project number 408062554 in the frame of the DFG/AiF-Cluster (CV) 6 “Physikalisches Management störender Schäume”.

Literature

Billet, R., Schultes, M., 1999: Prediction of Mass Transfer Columns with Dumped and Arranged Packings: Updated Summary of the Calculation Method of Billet and Schultes. Chem. Eng. Res. Des. 77:498-504

Winterburn, J. B., Martin, P. J., 2009: Mechanisms of ultrasound foam interactions. Asia-Pac. J. Chem. Eng. 4:184-190

Rodríguez G., Riera, E., Gallego-Juárez, J. A., Acosta, V. M., Pinto, A., Martínez, I., Blanco, A., 2010: Experimental study of defoaming by air-borne power ultrasonic technology. Physcs. Proc. 3: 135-139

Anderl, D., Bauer, M., Rauh, C., Rude, U., Delgado, A., 2014: Numerical simulation of adsorption and bubble interaction in protein foams using a lattice Boltzmann method. Food Funct. 5:755-763

Gallego-Juárez, J.A., Rodríguez, G., Riera, E., Cardoni, A., 2015: In: J. A. Gallego-Juárez and K. F. Graff: Power Ultrasonics. Oxford: Woodhead Publishing, 793-814

Vaidya, H. A., Ertunç, Ö., Lichtenegger, T., Hachmann, J., Delgado, A., Skupin, A., 2017: High-speed visualization of acoustically excited cavitation bubbles in a cluster near a rigid boundary. J. Visual-Japan 20:359-368

Gladbach, K., Delgado, A., Rauh, C., 2016: Modelling and Simulation of Food Foams. Proc. Appl. Math. Mech. PAMM 16:595-596

McHardy, C., Thünnesen, J., Horneber, T., Kostova, J., Hussein, M. A., Delgado, A., Rauh C., 2018: Active control of foams by physically based destruction mechanisms. Proc. Appl. Math. Mech. PAMM 18:e201800351

Thünnesen, J., Gatternig, B., Delgado A., 2019: Influence of high-performance ultrasound on beverage foams. Proceedings of 27. GALA-Fachtagung "Experimentelle Strömungsmechanik" 27:16.1 -16.8

Gatternig, B., Osorio Nesme, A., Almazán Torres, L., Thünnesen, J., Beck, T., McHardy, C., Delgado, A., 2019: Phenomena, mechanisms and structures in wished and unwished foams in matter of biological origin. In Proceedings of 2019 World Congress on Advances in Nano, Bio, Robotics, and Energy ANBRE19. Jeju Island, KR.

Wei, W., Xu, W., Deng, J., Tian, Z., Zhang, F., 2017: Free-surface air entrainment in open-channel flows. Sci. China Technol. Sc. 60:893-901

Roy, R. V., Schwartz, L. W., 1999: On the stability of liquid ridges. J. Fluid Mech. 39:293-318

Tran, T., de Maleprade, H., Sun, C., Lohse, D., 2013: Air entrainment during impact of droplets on liquid surfaces. J. Fluid Mech. 726:R3

Han, Z., Duan, L., Kang, Q. 2019: Behavior of a liquid drop in a rounded corner: Different contact angles. AIP Adv. 9:085203

Concus, P., Finn, R., McCuan, J., 2001: Liquid bridges, edge blobs, and Scherk-type capillary surfaces. Indiana Univ. Math. J. 50:411–441

Olenberg, A., Reschetnik, W., Kullmer, G., Kenig, E. Y., 2018: Optimization of structured packings using twisted tape inserts. Chem. Eng. Res. Des. 132:1-8

Sparrow, E. 1962: Laminar Flow in Isosceles Triangular Ducts. AIChE J. 8:599-604

Almazán, L., Osorio-Nesme, A., Delgado, A., 2019: Prevention or inhibition of foam formation through identification of non-existence domains in the interface in random and structured column-packings. Proceedings of 27. GALA-Fachtagung "Experimentelle Strömungsmechanik", 27:16.1 -16.8